

Synthesis of C_3N_4/MnO_2 Composite and Its Application in Supercapacitors

Junjia Wu^{1, a, *}, Wanying Zhang^{1, b}, Ailian Li^{1, c} and Qinghua Wang^{1, d}

¹The School of Chemistry, Chemical Engineering and the Environment, Minnan Normal University, China

^a1198155641@qq.com, ^b2176381053@qq.com, ^c1690813558@qq.com, ^dqhuawang@qq.com

Abstract

In this paper, $MnSO_4$, $KMnO_4$ and C_3N_4 were used as starting materials to synthesize C_3N_4/MnO_2 composite materials by hydrothermal method. The synthesized materials were characterized by X-ray diffraction analysis. The energy storage performances of the synthesized electrode materials were tested by galvanostatic charge-discharge test and cyclic voltammetry. The charge transfer kinetics of electrode materials was studied by electrochemical impedance spectroscopy. The effect of C_3N_4 on the electrochemical properties of MnO_2 electrode materials was studied in detail. The results show that the addition of C_3N_4 can significantly improve the specific capacitance, stability and charge storage capability of MnO_2 electrode material, which provides a new direction for the research of supercapacitors with better performance.

Keywords

C_3N_4/MnO_2 composite material; Supercapacitor; Electrochemistry; Specific capacitance.

1. INTRODUCTION

Since the 21st century, as the development of the economy and technology large amount of energy supplies are required. Nowadays, most of the energy consumed by the world is non-renewable fossil fuels. At present, we are facing the serious problem of increasing depletion of traditional fossil energy, and the human demand for renewable energy is becoming more and more urgent [1-3]. Therefore, sustainable energy storage technologies, such as supercapacitors with fast charge and discharge rate, high power density, and long cycle life, have attracted much attention [4-7]. In recent years, China has taken new energy vehicles as an important development goal of China in the future, which can not only save energy and reduce motor vehicle emissions, but also improve China's comprehensive strength. Therefore, the active development of supercapacitors as a green and sustainable energy storage device not only conforms to the trend of The Times, but also has a very high theoretical research and practical application value.

Supercapacitors can be divided into two categories: electrochemical double-layer capacitors and pseudocapacitors. Bilayer capacitors mainly use carbon materials with high surface area, which is the separation of charge at the interface between electrode and electrolyte [8]. Pseudocapacitors are based on surface or near-surface two-phase redox reactions involving conductive polymers and transition metal oxides such as polyaniline, polypyridine, MnO_2 and RuO_2 class. Transition metal oxides can store the charge through rapid, reversible redox reactions, with very high theoretical specific capacitance values. Among them, MnO_2 has the advantages of high abundance, wide potential window, green environmental protection, low cost, etc., and has been widely studied in the field of supercapacitors. MnO_2 is a kind of

traditional electrode material for pseudo-capacitors and batteries [9]. It has rich crystalline phase structure, fast access channels for electrolyte ions, and high theoretical specific capacity. Due to the variety of variable valence states of manganese, it has excellent ion storage performance. However, the low ionic and electronic conductivity of MnO_2 limits its pseudo-capacitor charge storage mechanism by the surface layer [10]. Although the theoretical specific capacity of the MnO_2 supercapacitor is high, its experiments have fallen far short of expectations. At high charge and discharge rates, the capacity of MnO_2 supercapacitors is reduced, the conductivity is poor, and the cycle stability is poor, which limits its development [11, 12]. In order to study new materials with better properties, an important method is to combine different materials to form composite materials, because there is a synergistic effect between different materials, which can overcome the disadvantages of a single material and reflect better advantages [13]. C_3N_4 is a two-dimensional semiconductor material with good thermal and chemical stability, which is stable at high temperature. The thermal stability starts to decline after 600°C , and the performance can be kept stable under strong acid and alkali environment. By synthesizing binary composites with C_3N_4 , the ion transport conductance of MnO_2 electrode materials can be improved. C_3N_4 is considered as a promising pseudocapacitor material due to its easy synthesis, low cost and remarkable high environmental stability. The addition of g- C_3N_4 can significantly resolve the problem of MnO_2 , improve the specific capacitance and stability of the electrode material, and provide a new direction for the research of supercapacitors with better performance.

2. EXPERIMENTAL

2.1. Instruments and reagents

CHI660E Electrochemical Workstation (Shanghai Chenhua), CT2001A battery tester (Wuhan Blue Electric), Ultima IV XRD diffractometer (Japan science).

Urea, $\text{MnSO}_4\cdot\text{H}_2\text{O}$, KMnO_4 , Na_2SO_4 were purchased from Xilong Chemical Co., LTD; N-methylpyrrolidone, polyvinylidene fluoride (PVDF) purchased from Aladdin Industrial Company.

2.2. Preparation of the electrode material

2.2.1 Preparation of g- C_3N_4

10.0 g of urea was put in an alumina crucible and wrapped in tin foil, and then heated at 550°C for 4 h in a tubular furnace with heating rate of 5°C min^{-1} . After the reaction, remove the crucible after cooling. The samples were removed, the products were fully washed with water in a sand core funnel, and dried at 80°C under vacuum for 12 h to obtain the yellow powder g- C_3N_4 .

2.2.2 Hydrothermal synthesis of $\text{C}_3\text{N}_4/\text{MnO}_2$ composite

$\text{MnSO}_4\cdot\text{H}_2\text{O}$ 1.352 g (8 mmol), KMnO_4 1.264 g (8 mmol), G- C_3N_4 0.02 g (2 mmol) were placed in a 100 mL beaker, 80 mL deionized water (DI) were then added into the beaker. The mixer were stirred with a magnetic stirrer for 2 h at the speed of 200 r/min to obtain a homogenous solution with an initial concentration of 0.1 mol/L [4]. The solution was then put into a 100 ml a PTFE autoclave and reacted at 150°C for 24 h. After the reaction the samples were extracted and washed with deionized water for several times, and dried in a vacuum drying oven at 60°C for 8 h to obtain dark brown $\text{C}_3\text{N}_4/\text{MnO}_2$ powder (1.481g).

A control MnO_2 sample was prepared in a similar procedure, except that none C_3N_4 was added during synthesizing.

2.2.3 Preparation of electrode sheets

8 mg C_3N_4/MnO_2 , 1 mg carbon black, 200 μ L N-methylpyrrolidone (NMP) and 10 μ L polyvinylidene fluoride (PVDF, 5% in NMP) were mixed and ground for 10 min in a agate mortar. The paste was covered on three pieces of nickel foam (NF) with an active area of 1×1 cm^2 . The coated NFs were then dried at 60 $^\circ$ C under vacuum for 8 h. After drying, the NFs were pressed under 10 MPa for 30s. The MnO_2 electrode sheet was prepared by the same method. The active material load is approximately 2 mg.

2.3. Electrochemical test

CHI660E electrochemical workstation was used to conduct relevant tests to study the electrochemical properties of the samples. The main electrochemical performance testing methods include cyclic voltammetry (CV), galvanostatic charge-discharge method (GCD), Electrochemical impedance spectroscopy (EIS), stability test, etc. The electrochemical test was conducted in a three-electrode mode. In the three-electrode system, the working electrode is nickel foam coated with C_3N_4/MnO_2 or MnO_2 active substance, the reference electrode is saturated Ag/AgCl electrode, the opposite electrode is platinum wire, and the electrolyte solution is 1 mol/L Na_2SO_4 solution.

The currents for the GCD tests are 1~10 mA/ cm^2 , and the voltage range is 0~1 V. According to the GCD test results, the mass based capacitance C_m (F/g) of the capacitor can be calculated as follows:

$$C_m = \frac{I \times \Delta t}{m \times \Delta V} \quad (1)$$

The calculation formula of the areal capacitance C_A (mF/ cm^2) is as follows:

$$C_A = \frac{I \times \Delta t}{A \times \Delta V} \quad (2)$$

Where: I (A) is the discharge current, m (g) is the mass of the active material of the electrode material, Δt (s) is the discharge time, ΔV (V) is the voltage window, and A (cm^2) is the area of the effective electrode.

EIS was conducted by a three-electrode system with an applied voltage amplitude of 5 mV and an initial potential of 0V in a frequency range of $10^{-2} \sim 10^5$ Hz.

2.4. X-Ray Diffraction Analysis (XRD)

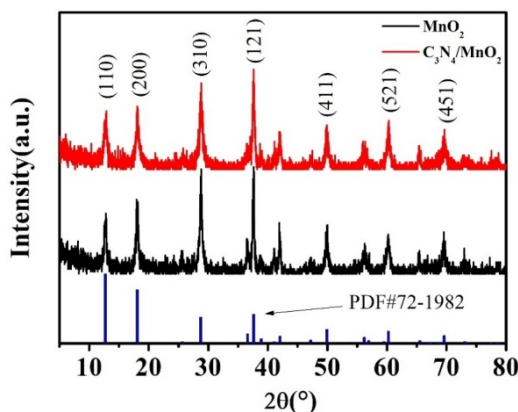


Figure 1. X-ray diffraction patterns of C_3N_4/MnO_2 composite and MnO_2

The prepared C_3N_4/MnO_2 and MnO_2 materials were characterized by X-ray diffraction (XRD) to determine their phase structures. Figure 1 shows the X-ray diffraction pattern of C_3N_4/MnO_2 material and MnO_2 material, which belongs to the tetragonal system MnO_2 (PDF#72-1982). Seven sharp diffraction peaks appear at 2 theta 12.74° , 18.06° , 28.73° , 37.62° , 49.89° , 60.24° and 69.60° , respectively, which corresponding to the (110), (200), (310), (121), (411), (521) and (451) crystal planes of the tetragonal phase MnO_2 . These results indicate that MnO_2 with high purity and high crystallinity has been synthesized by hydrothermal reaction. There is no obvious difference between the X-ray diffraction patterns of C_3N_4/MnO_2 material and MnO_2 material. We believe this is caused by two factors: on one hand, the amount of added C_3N_4 is small; on the other hand, the diffraction peak (220) of MnO_2 near 26° is close to the characteristic diffraction peak (002) of C_3N_4 , which will mask the latter. Therefore, no significant diffraction peak of C_3N_4 can be observed in the C_3N_4/MnO_2 composite .

2.5. Cyclic Voltammetric Test

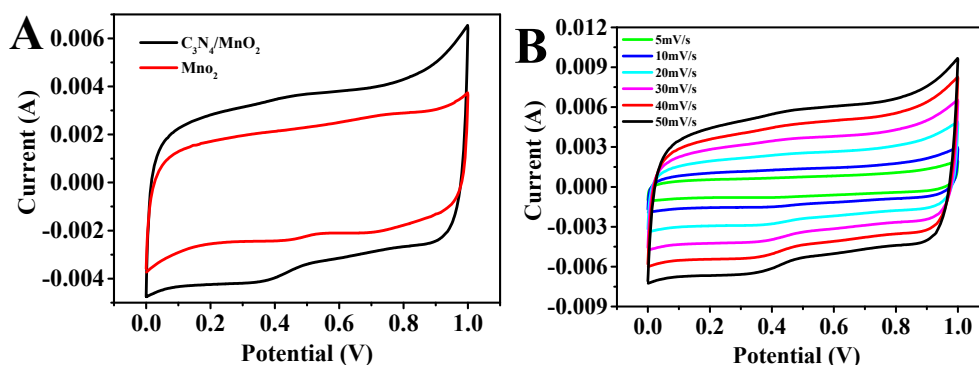


Figure 2. (A) Cyclic voltammetry curves of C_3N_4/MnO_2 and MnO_2 materials at a scanning rate of 30 mV/s; (B) cyclic voltammetry curve of C_3N_4/MnO_2 material at scanning rates of 5 ~ 50 mV/s;

In order to study the electrochemical energy storage properties of C_3N_4/MnO_2 composites, C_3N_4/MnO_2 and MnO_2 materials were used as working electrodes for electrochemical performance testing. The three-electrode system was tested with 1 mol/L Na_2SO_4 as electrolyte, nickel foam as working electrode, Ag/AgCl electrode as reference electrode and platinum wire as electrode.

Firstly, cyclic voltammetry curve was tested, and the results were shown in Figure 2. It can be seen from Figure 2 (A) that under the condition of 30 mV/s sweep speed, the enclosed area of the cyclic voltammetric curve with C_3N_4/MnO_2 as the electrode material is obviously larger than that of MnO_2 , indicating that the specific capacitance of C_3N_4/MnO_2 material is larger. Although manganese dioxide is considered to be a promising electrode material, C_3N_4 and MnO_2 have poor electrical conductivity. By preparing C_3N_4/MnO_2 composites, the defects of both can be significantly diminished. C_3N_4 can be easily composited with other compounds, and has good crystallization properties conducive to charge transfer, as well as better chemical and thermal stability [17]. Therefore, the addition of C_3N_4 is conducive to improving the electrochemical performance of MnO_2 electrode.

Figure 2 (B) shows the cyclic voltammetry curves of C_3N_4/MnO_2 composites and MnO_2 materials in 1 mol/L Na_2SO_4 solution with various sweep speed. In the sweep speed range of 5 ~ 50 mV/s, the CV curves show good symmetry, and all of them are rectangular-like, indicating that the C_3N_4/MnO_2 composite electrode exhibits double-layer capacitance. The CV curves does not show obvious deformation as the the sweep speed increases, indicating that the C_3N_4/MnO_2 composite electrode has good rate capability at high scan rate.

2.6. Galvanostatic current charge and discharge curve

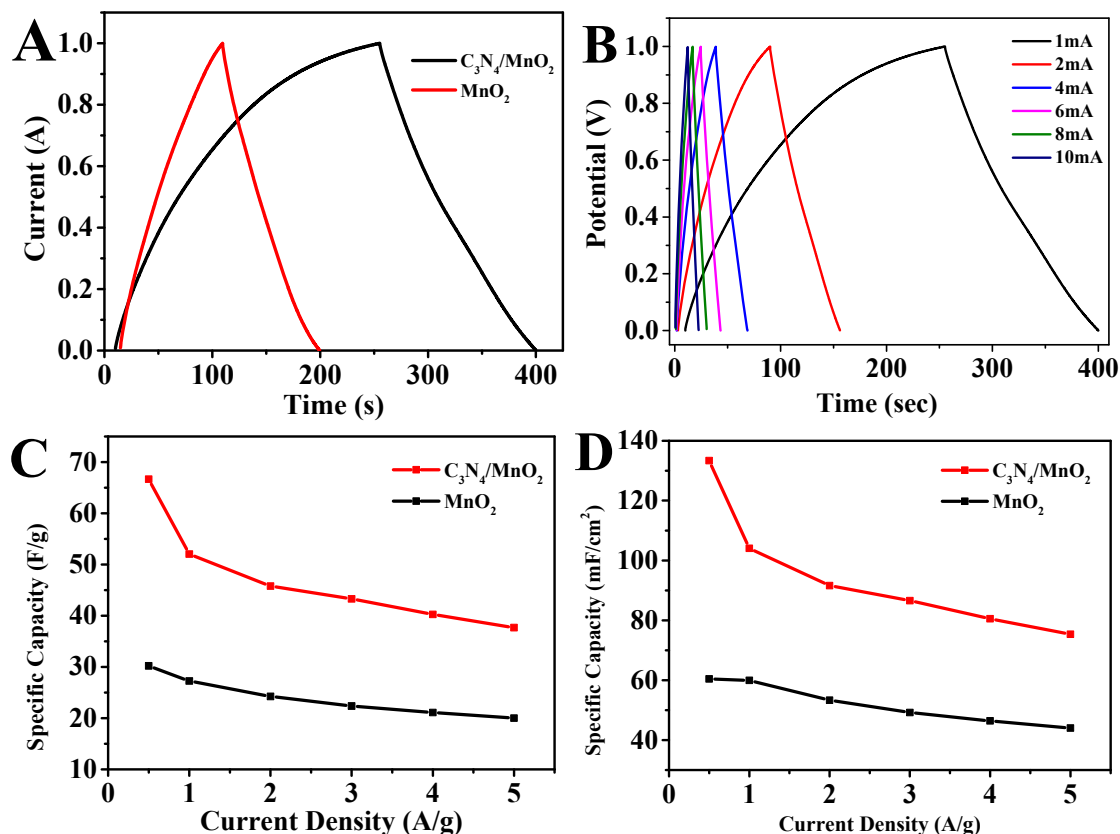


Figure 3. (A) GCD curves of electrodes C_3N_4/MnO_2 and MnO_2 at a current of 0.5 A/g; (B) GCD curves of C_3N_4/MnO_2 at current densities ranging from 0.5 to 5 A/g; (C) mass based specific capacitance at various current densities of C_3N_4/MnO_2 and MnO_2 ; (D) areal capacitance of C_3N_4/MnO_2 and MnO_2 at various current densities.

The GCD curves of C_3N_4/MnO_2 composites and MnO_2 materials were measured in a three-electrode system. Figure 3 shows the charge and discharge curves of C_3N_4/MnO_2 composites and MnO_2 materials at different current densities, and the specific capacitance of the active substance can be calculated according to formula (2).

Figure 3(A) compares the GCD curves of the C_3N_4/MnO_2 electrode and the MnO_2 electrode at a current density of 0.5 A/g in a voltage range of 0 to 1 V. Clearly, the discharge time of the C_3N_4/MnO_2 composite electrode can reach 150 s, while that of the MnO_2 electrode is only 90 s. The discharge time of the C_3N_4/MnO_2 composite electrode is longer than that of the MnO_2 electrode, which means that the C_3N_4/MnO_2 electrode has a higher specific capacitance than the MnO_2 electrode. According to formula (3) and (4), the mass specific capacitance (F/g) of the two electrode materials is 200.05 F/g and 90.64 F/g, while and the areal capacitance (mF/cm²) is 400.10 mF/cm² and 181.27 F/cm², respectively, at a current density of 0.5 A/g.

Figure 3 (B) compares the GCD curves of MnO_2/C_3N_4 electrodes at various current densities. At the current density of 0.5~5A/g, these curves are close to the isosceles triangle, indicating that the charging time and discharge time are close, indicating good reversibility in the charging and discharging process. Figure 3 (C) and (D) shows the comparison of specific capacitances of C_3N_4/MnO_2 composites and MnO_2 materials at different current densities calculated according to formula (3) and (4). As the current density increases, the specific capacitances of both materials tend to decrease. As the current density increases from 0.5 to 5 A/g, the specific capacitance of C_3N_4/MnO_2 electrode material decreases from 200.01 F/g to 113 F/g with a

retention rate of 60.3%. The C_3N_4/MnO_2 composites exhibits larger specific capacitance at all current densities than that of MnO_2 .

2.7. Electrochemical impedance spectra

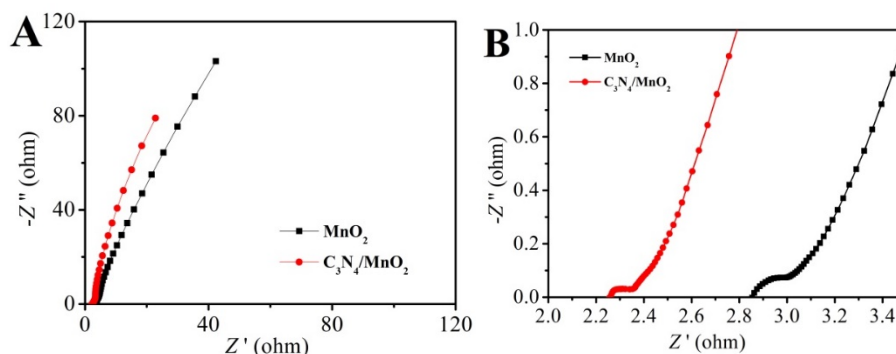


Figure 4. (A) Nyquist curves of C_3N_4/MnO_2 and MnO_2 in three-electrode system; (B) magnification of the high frequency region.

AC impedance test is when the electrode system is disturbed by a sinusoidal AC signal of voltage or current, the impedance or admittance of the electrode can be obtained from the corresponding current or voltage response signal. The electrochemical impedance spectra (EIS) can be obtained from these signals. The high frequency region is the dynamic controlled region with a semicircular profile, while the low frequency region is the diffusion controlled region with a straight line profile. The region between the high frequency region and the low frequency region is the mixed control region.

Figure 4 shows the EIS curves of C_3N_4/MnO_2 composites and MnO_2 materials. The slope of the line at low frequency region indicates the speed at which ions diffuse from solution to electrode surface. As shown in figure 4(A), the C_3N_4/MnO_2 composite displays a larger slope than that of MnO_2 , indicating a faster ion transfer kinetics. Figure 4(B) shows the amplification of the high frequency region of the EIS curve. Semicircles can be clearly identified in the high frequency region of the EIS curve, the diameters of which equal to the interface charge transfer resistance (R_{CT}) of the electrodes. Obviously, the C_3N_4/MnO_2 composite material displays a smaller semicircle than that of MnO_2 , indicating that the composite has a smaller R_{CT} . The intercept of the EIS curve with the Z' axis in the high frequency region corresponds to the equivalent series resistance (R_s). The R_s of the C_3N_4/MnO_2 composite is about 2.25Ω , which is smaller than that of 2.8Ω for MnO_2 . The EIS results demonstrate that the C_3N_4/MnO_2 composite has a faster charges transfer kinetics and better electrical conductivity than MnO_2 .

2.8. Stability test

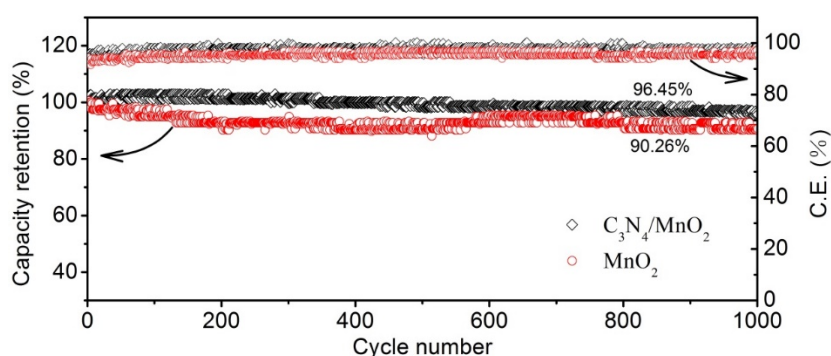


Figure 5. GCD cycle stability test of C_3N_4/MnO_2 composite (A) and MnO_2 material (B) at a current density of $1 A/g$

Long-term cycle stability is an important index to measure the practical application of supercapacitors. GCD cycle tests were conducted for C_3N_4/MnO_2 and MnO_2 materials at a current density of 1 A/g, with the results shown in Figure 5. The C_3N_4/MnO_2 composite material shows a very slow decline trend within 1000 GCD cycles with a high average coulomb efficiency close to 99%, and the capacitance retention ratio is 96.45% versus the initial value. On the other hand, the MnO_2 electrode showed a faster decline trend than the composite electrode, the capacitor retention ratio is 90.26%. The average coulomb efficiency for MnO_2 electrode is close to 97%, which is smaller than that of C_3N_4/MnO_2 composite. It can be seen that the C_3N_4/MnO_2 composite electrode material exhibits better electrochemical stability and reaction reversibility than the single MnO_2 material.

3. CONSLUSION

In summary, C_3N_4/MnO_2 composite and MnO_2 materials were prepared by hydrothermal method and characterized by X-ray diffraction analysis. The electrochemical energy storage performance of the electrode materials was tested by GCD, CV and AC impedance tests, and the long-term performance stability of the materials was studied by GCD cycles test.

Through our experiments, we found that the addition of C_3N_4 can significantly improve the specific capacitance, stability and ion diffusion kinetics of electrode material. The GCD cycle stability test revealed that C_3N_4/MnO_2 composite material exhibits smaller capacity degradation and higher coulomb efficiency. Compared with the MnO_2 material without C_3N_4 , energy storage performance of C_3N_4/MnO_2 composite has been greatly improved in all aspects, which provides a new idea for the research of high-performance electrode material for supercapacitors.

ACKNOWLEDGMENTS

This research is supported by the college student innovation and entrepreneurship project of Fujian province (S202210402013).

REFERENCES

- [1] Zhao Y. et al. Wood-inspired morphologically tunable aligned hydrogel for high-performance flexible all-solid-state supercapacitors. *Adv. Funct. Mater.* 2020, 1909133.
- [2] Tiantian Tiantian, calamus carbon.C/MnO2 Preparation of Composites and their Application in SuperCapacitors, 2021, Tianjin University.
- [3] Hao, J. et al. Deeply understanding the Zn anode behaviour and corresponding improvement strategies in different aqueous Zn-b/ased batteries. *Energy & environmental science*, 2020. 13(11): 3917-3949.
- [4] Shanbhag, D. et al. Hydrothermally synthesized reduced graphene oxide and Sn doped manganese dioxide nanocomposites for supercapacitors and dopamine sensors. *Materials Today Energy*, 2017. 4: 66-74.
- [5] Gao Bang. MoO_2/C Preparation and Electrochemical properties of nanofiber Supercapacitors, 2020, Taiyuan University of Technology.
- [6] Yang Hongsheng, Zhou Xiao, Zhang Qingwu. Electrochemical properties of supercapacitors with multilevel polypheniline particles as electrode active material. *Journal of Physical Chemistry*, 2005.21 (4): 414-418.
- [7] Zhang, T. et al. Fundamentals and perspectives in developing zinc-ion battery electrolytes: a comprehensive review. *Energy & environmental science*, 2020. 13(12): 4625-4665.

- [8] Zhang, N. et al. Three-Dimensional Pompon-like MnO₂/Graphene Hydrogel Composite for Supercapacitor. *Electrochimica acta*, 2016. 210: 804-811.
- [9] Song J. Facile Synthesis of MnO₂@attapulgite Nanoparticles for Supercapacitor. *International Journal of Electrochemical Science*, 2020. 9(15): 9378-9391.
- [10] Kong Lingyu, et al. Preparation of MnO₂-rGO / bamboo cellulose-based carbon aerogel and its application in supercapacitors. *Journal of Composite Materials*, 2022.39 (03): 1268-1279.
- [11] Marquardt, R.M.Quack. *Physical Chemistry and Chemical Physics: A survey*, in Reference Module in Chemistry, Molecular Sciences and Chemical Engineering.2013, Elsevier.
- [12] Liu Wei shuai. *The 3D porous FeC₂O₄/ Graphene and MnO₂/ Preparation of graphene electrode materials and applications in Supercapacitors*, 2018, University of Science and Technology of China.
- [13] Hong Congcong. *MnO₂ Research on the Preparation and Electrochemical properties of Base Supercapacitors*, 2018, Zhejiang Sci-Tech University.
- [14] Guo Huilin et al. Analysis and discussion of cyclic voltammetry principle. *University Chemistry*, 2023:1-8.
- [15] Chen Lina et al. Research progress of drainage zinc ion battery. *Journal of Inorganic Materials*, 2017.32 (03): 225-234.
- [16] Khani, H.and D.O.Wipf, Iron Oxide Nanosheets and Pulse-Electrodeposited Ni-Co-S Nanoflake Arrays for High-Performance Charge Storage. *ACS applied materials & interfaces*, 2017. 9(8): 6967-6978.
- [17] Canal source.g-C₃N₄/ Research on the preparation and properties of graphene-based flexible supercapacitors, 2020, Changchun University of Technology.62.